Chapter 8

Advanced Polymer-Surfactant Systems via Self-Assembling

Laura Romero-Zerón and Xingzhi Jiang

Additional information is available at the end of the chapter

http://dx.doi.org/10.5772/intechopen.74618

Abstract

This chapter summarizes the formulation of supramolecular polymers built via noncovalent and β-cyclodextrin (β-CD) host-guest interactions. The self-assembling polymeric (SAP-AP) systems were formulated by mixing associative polymers with an anionic surfactant and β-CD. These SAP-AP systems were characterized by rheological analysis and several techniques to establish their stability under mechanical shear, high ionic strength, and high temperature. The experimental results demonstrate that the SAP-AP systems display enhanced viscoelastic properties, shear stability, superior structural strength, and tolerance to high-salinity brines relative to the corresponding baseline polymers.

Keywords: self-assembling, β-CD host-guest complexations, noncovalent bonding, structural regeneration, self-healing, self-repairing, associating polymers, supramolecular systems, functional polymers

1. Introduction

The chemistry of polymers for applications in enhanced oil recovery (EOR) has been advanced to improve their stability and functionality at elevated temperatures and in brines containing high salinity and hardness concentration (i.e. harsh reservoir conditions). Therefore, a variety of functional moieties have been attached to the polymer structure including: salt-tolerant and hydrolysis-resistant moieties such as allyl sulfonic acid, 2-acrylamido-2-methylpropane sulfonate (AMPS), and/or n-vinyl pyrrolidone (n-VP) monomers; hydrophobic groups like n-alkyl (i.e. $\geq C_6$ carbon numbers) acrylamide, and styrene; ring structures and large-rigid side groups to improve the shear stability such as styrene sulfonic acid, n-alkyl maleimide, acrylamide-base long-chain alkyl acid, and 3-acrylamide-3-methyl butyric acid, among others [1–6].

This work evaluated the generation of advanced polymer-surfactant systems built via noncovalent and host-guest interactions based on β-cyclodextrin that would be stable under harsh reservoir conditions. The aim was to formulate efficient, chemically stable, and cost-effective systems as an alternative to expensive chemical synthesis.

Self-assembly allows the coassembly of two or more types of building blocks, resulting in increasingly structurally complex nanoassemblies that may have physical and chemical properties that are distinct from those of the original monostructures [7]. Host-guest interactions refer to the formation of supramolecular inclusion complexes based on macrocyclic molecules (i.e. host molecules) consisting of two or more entities connected via noncovalent interactions in a highly controlled and cooperative manner. These host-guest inclusions are relatively stable and provide reliable and robust connections for the fabrication of stimuli-responsive supramolecular systems [8]. Cyclodextrins (CDs) are the most used and affordable hosts in the field of inclusion chemistry [7, 9, 10].

Supramolecular β-CD-based polymer systems retain their structural stability and functionality (i.e. self-healing) after exposure to externally applied stimuli or shear forces increasing the life span of these materials [8, 7]. The self-healing capability is highly dependent on the noncovalent connections in the polymer backbone and on the decomplexation and complexation of the supramolecular system [7, 8, 11, 12]. Therefore, supramolecular chemistry built on weak and reversible noncovalent interactions has emerged as a powerful and versatile strategy to design and fabricate materials with extraordinary reversibility and adaptivity with potential applications in diverse fields [8].

In this chapter, we first discuss the steps followed during the formulation of the SAP-AP systems and their rheological analysis. Secondly, we explore the effect of ionic strength on the rheological properties of the SAP-AP systems. Next, we discuss the combined effect of shear and ionic strength on the structural stability of the self-assembling systems. Finally, we summarize the short- and long-term thermal performance of the SAP-AP systems.

2. Formulation of self-assembling systems

The associating polymers (APs) were provided by SNF Holding Co. (Riceboro, Georgia, USA). Two of these APs, designated as AP1 and AP2, display high grade of anionicity (hydrolysis degree: 25 – 30 mol% at room temperature) and high molecular weights (≈16 – 20 million Dalton). AP1 has a low hydrophobic content, while AP2 has a medium hydrophobic content. The third associating polymer, designated as AP3, has low anionicity (hydrolysis degree: 15 mol%), low molecular weight (8 – 12 million Dalton), and high hydrophobic content [6, 13, 14]. The relative hydrophobic contents of AP1, AP2, and AP3 are 1, 2, and 5 – 6, respectively [13]. APs are tolerant to high salinities at moderate temperatures [14]. The anionic surfactant, a primary alcohol alkoxy sulfate 30% active, was supplied by Sasol North America (Houston, Texas) [15]. β-Cyclodextrin (β-CD) Technical Grade Trappsol® was acquired from Cyclodextrins Technology Development Inc. (CDT, Inc. Alachua, Florida, USA). The assay of the β-CD powder was 98% (molecular weight: 1135 g/mol).

The SAP-AP systems were formulated in synthetic reservoir brines [16] and the effect of different concentrations of brine on the rheological properties of the SAP-AP systems was determined. **Table 1** shows the compositions of the synthetic brines.

The formulation of the SAP-AP systems was based on a molar ratio of surfactant to β-CD of 2:1 established from our previous research [17–20]. In the initial formulation of the SAP-AP system, the concentration of polymer was kept fixed at 0.5 wt% in 2.1 wt% brine. **Table 2** presents the experimental design applied for the SAP-AP formulation. All the experiments were duplicated or even triplicated, and the results presented are the average of several measurements.

Self-assembly was monitored through rheology by observing the changes in the elastic (G') and viscous behavior (G''), loss factor ($\tan\delta = G''/G'$), and complex viscosity, $|\eta^*|$, relative to the baseline associating polymers [8–10, 12, 21]. The rheological analysis was conducted using a Bohlin Gemini HR Nano Rheometer manufactured by Malvern (Worcestershire,

Components	**Total concentration (wt% or TDS)**				
	1.40	**2.10**	**4.21**	**6.31**	**8.41**
NaCl	1.15	1.72	3.45	5.17	6.9
$MgCl_2$	0.03	0.04	0.09	0.13	0.18
$CaCl_2$	0.22	0.33	0.65	0.98	1.30
Na_2SO_4	0.01	0.01	0.02	0.03	0.04

Table 1. Synthetic brine compositions.

Surfactant (ppm)	**β-CD concentration (ppm)**					
	0	**30**	**50**	**70**	**90**	**110**
0	Baseline-*AP	β-CD-AP	β-CD-AP	β-CD-AP	β-CD-AP	β-CD-AP
30	**S 30-AP	***SAP-AP AP 30				
50	S 50-AP		SAP-AP S/β-CD50			
70	S 70-AP			SAP-AP S/β-CD70		
90	S 90-AP				SAP-AP S/β-CD90	
110	S 110-AP					SAP-AP S/β-CD110

*AP: associating polymer: AP1, AP2, or AP3 mixed at a fixed concentration of 0.5 wt%.
**S: surfactant.
***SAP-AP: self-assembling polymeric system.

Table 2. Experimental design: SAP-AP formulations.

UK) equipped with parallel-plate measuring geometry (gap between the plates of 1000 μm) and solvent trap to avoid evaporation and/or drying effects. First, amplitude sweeps were run to determine the limit of the linear viscoelastic (LVE) range of the samples at 25°C; followed by frequency sweeps to establish the time-dependent deformation behavior [22]. G', G'', tanδ (G''/G'), and $|\eta^*|$ were plotted as a function of the angular frequency (ω) in logarithmic scales on both axis.

2.1. Effect of β-CD addition

Figure 1 displays the results of the oscillatory tests for β-CD/polymer blends at different β-CD concentrations and fixed concentration of polymer (0.5 wt%). **Figure 1(a–c)** corresponds to formulations using polymers AP1, AP2, and AP3, respectively. **Figure 1(a–c)** indicates that the addition of different concentrations of β-CD did not improve the frequency-dependent function of the baseline polymers; on the contrary, the addition of β-CD makes these polymers more inflexible and rigid. In all cases, tanδ increases, while G' and G'' decrease relative to the baseline polymers.

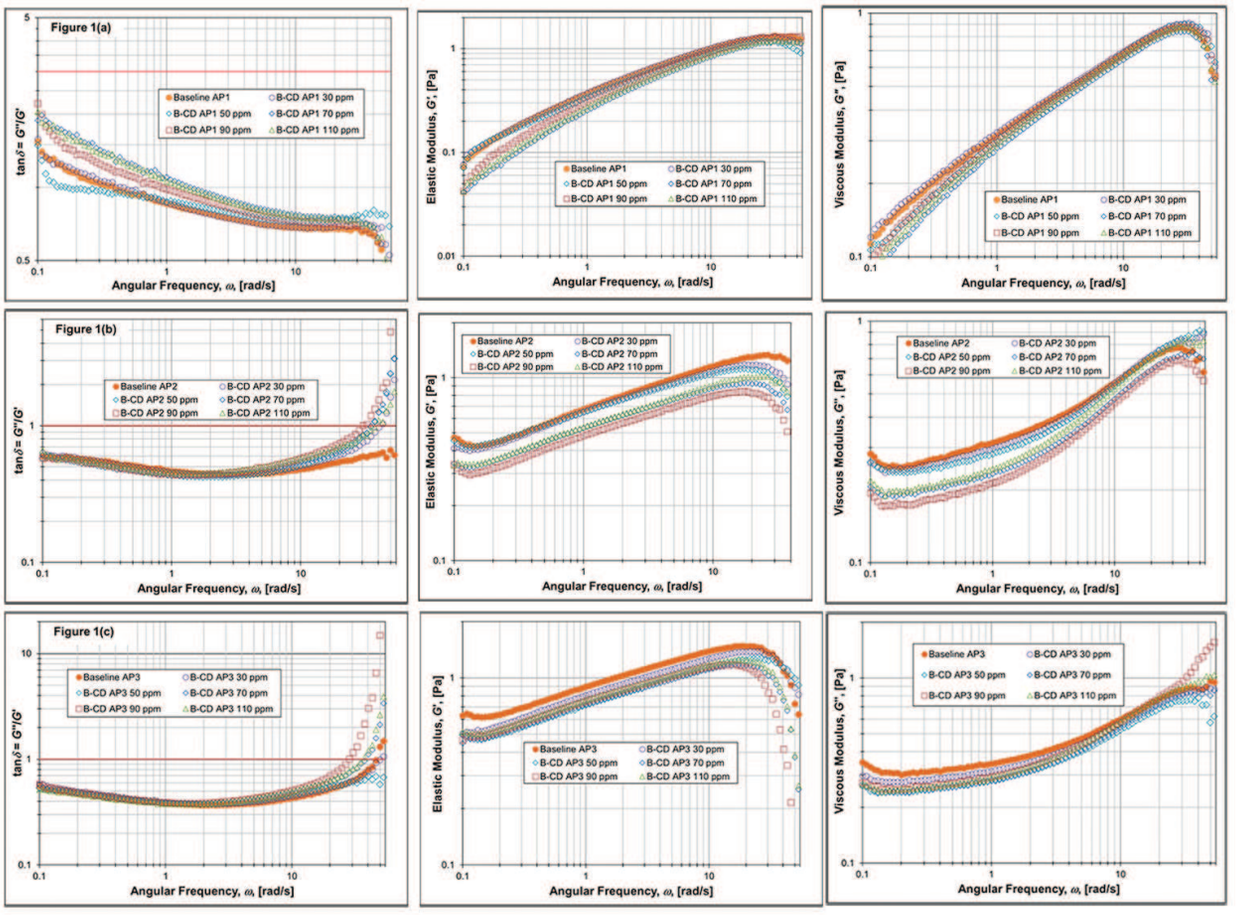

Figure 1. Oscillatory tests for β-CD/polymer blends at different β-CD concentrations at 0.5 wt% polymer solution in 2.1 wt% brine.

2.2. Effect of surfactant addition

Figure 2(a–c) demonstrates the effect of the addition of surfactant on the viscoelastic properties of polymers AP1, AP2, and AP3. These plots reveal interactions (noncovalent associations) among the surfactant and polymers AP1, AP2, and AP3. The addition of surfactant increases the elasticity (tanδ decreases and G' increases) and viscosity of the samples (G'' and $|\eta^*|$ increase) relative to the respective baseline polymers. However, these plots also indicate that there is no a clear relationship between surfactant concentration and the improvement of the viscoelastic properties. For instance, the surfactant concentrations that render the best viscoelastic properties for surfactant-AP1 ranged from 30 to 70 ppm; for surfactant-AP2 was 70 ppm, and for surfactant-AP3 ranged from 30 to 90 ppm.

2.3. Effect of the simultaneous addition of surfactant and β-CD

Figure 3(a–c) demonstrates that the simultaneous addition of surfactant and β-CD produces strong noncovalent interactions and robust self-assembling. Self-aggregation significantly increases the viscoelastic properties of the different systems, specifically for the SAP-AP systems formulated using polymers AP2 (**Figure 3(b)**) and AP3 (**Figure 3(c)**). Furthermore, the

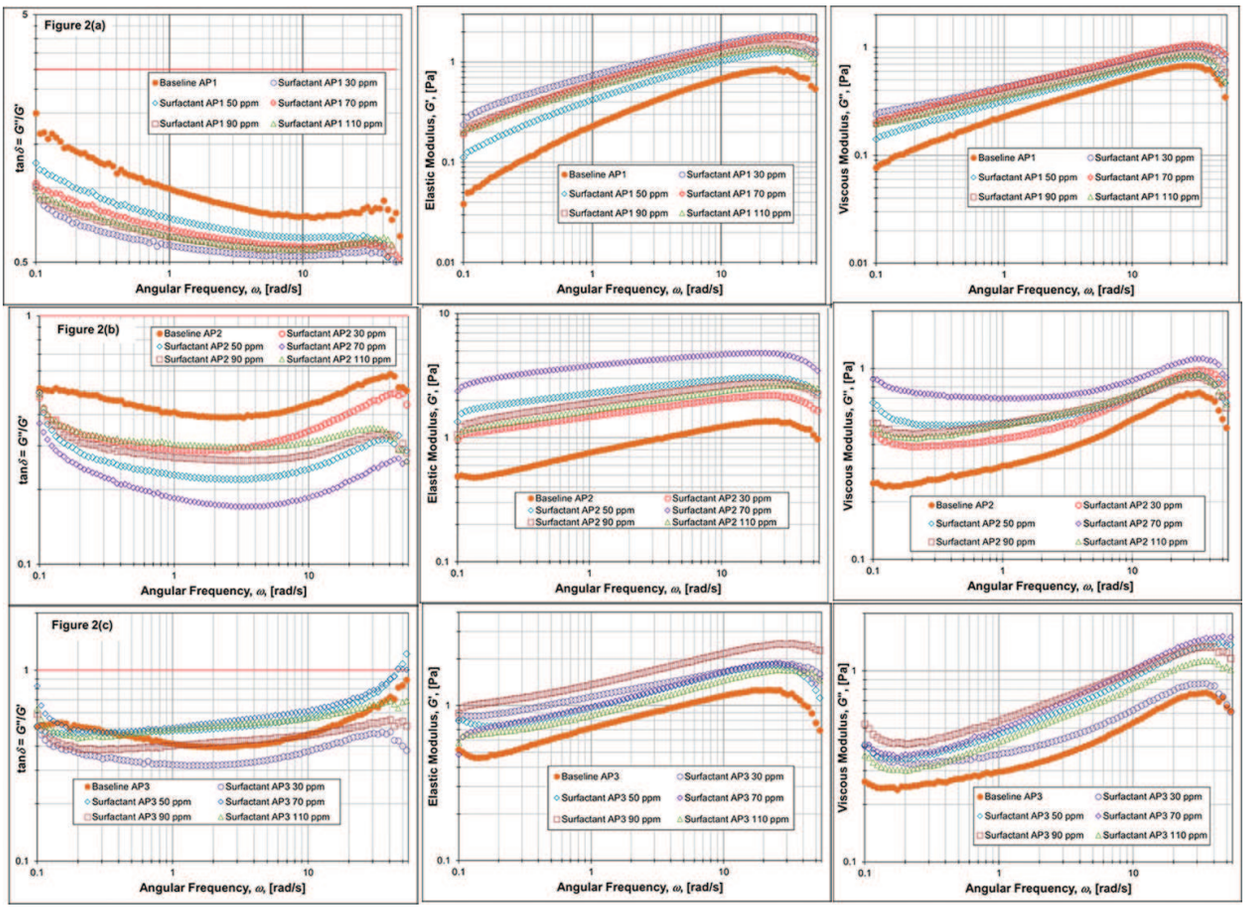

Figure 2. Oscillatory tests for surfactant/AP blends at different surfactant concentrations at 0.5 wt% polymer solution in 2.1 wt% brine.

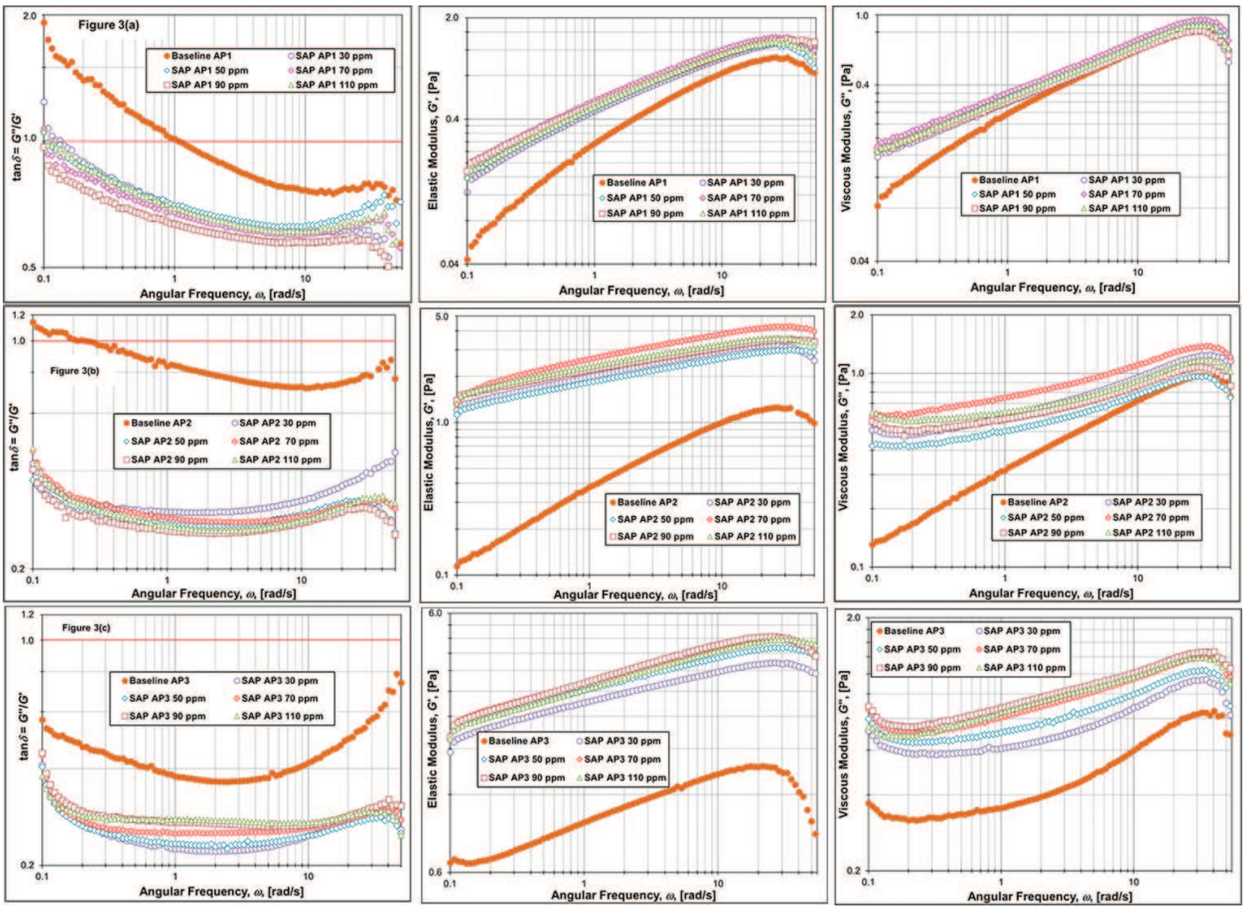

Figure 3. Oscillatory tests for surfactant/β-CD/AP blends at different surfactant/β-CD concentrations at 0.5 wt% polymer solution in 2.1 wt% brine.

experimental results show a clear and consistent relationship between surfactant/β-CD concentration and the improved viscoelastic properties of the SAP-AP systems. The self-assembling systems displaying the most enhanced viscoelasticity were obtained at a surfactant concentration of 70 ppm and β-CD concentration of 70 ppm (**Figure 3(a–c)**). The viscoelastic properties achieved by the SAP-AP systems at a surfactant/β-CD concentration of 70 ppm overlapped the viscoelastic performance corresponding to surfactant/β-CD concentrations of 90 and 110 ppm; therefore, a surfactant/β-CD concentration of 70 ppm was selected as the optimum concentration from the technical and cost-effective standpoint.

All the self-assembling systems display a decrease of the loss factor (tanδ), which indicates that these SAP-AP systems are more elastic (i.e. improved reversible deformation behavior) relative to the baseline AP polymers. This observation agrees with the significant increase of G' shown by the SAP-AP systems, especially for the SAP-AP2 with a percentage increase of G' = 310% and the SAP-AP3 with a percentage increase of G' = 220%. Likewise, the loss modulus (G'') and the complex viscosity ($|\eta^*|$) increased significantly. For instance, the SAP-AP2 shows a percentage increase of G'' = 61% and of $|\eta^*|$ = 253%; while the SAP-AP3 displays a percentage increase of G = 694% and of $|\eta^*|$ = 414%.

The remarkable gain of viscoelastic properties achieved by these SAP-AP systems is attributed to self-association through β-CD host-guest interactions and other noncovalent interactions (i.e. hydrogen bonding and hydrophobic interactions, among others). These observations agree with previous research in which self-aggregation through intermolecular noncovalent associations increased solution viscosity [7].

In this work, only 70 ppm (0.007 wt%) of surfactant and 70 ppm (0.007 wt%) of β-CD were added to the AP polymers dissolved in brine. β-CD rapidly forms inclusion complexes with various hydrophobic guest moieties and polymeric chains [7]. The hydrophobic pendant groups from the associating polymers and the hydrophobic tails of the surfactant are typical guest moieties that can be spontaneously included into the β-CD cavity through both faces: the primary and secondary faces. While the hydrophilic end (i.e. polar part) of the anionic surfactant can interact with the hydrophilic pendant groups (i.e. amide groups contained in the associating polymers) through hydrogen bonding (i.e. H-bridges) or with the carboxylate pendant groups of the polymer backbone via electrostatic interactions through divalent cation-bridges (i.e. Ca^{2+} or Mg^{2+}) present in the brine.

Figure 4 displays a hypothetical network structure formed through self-assembly. This 3D supramolecular structure is responsive and reversible because these physical bonds are not rigid [22]. Furthermore, the resulting high-order macromolecule displays increased hydrophilicity

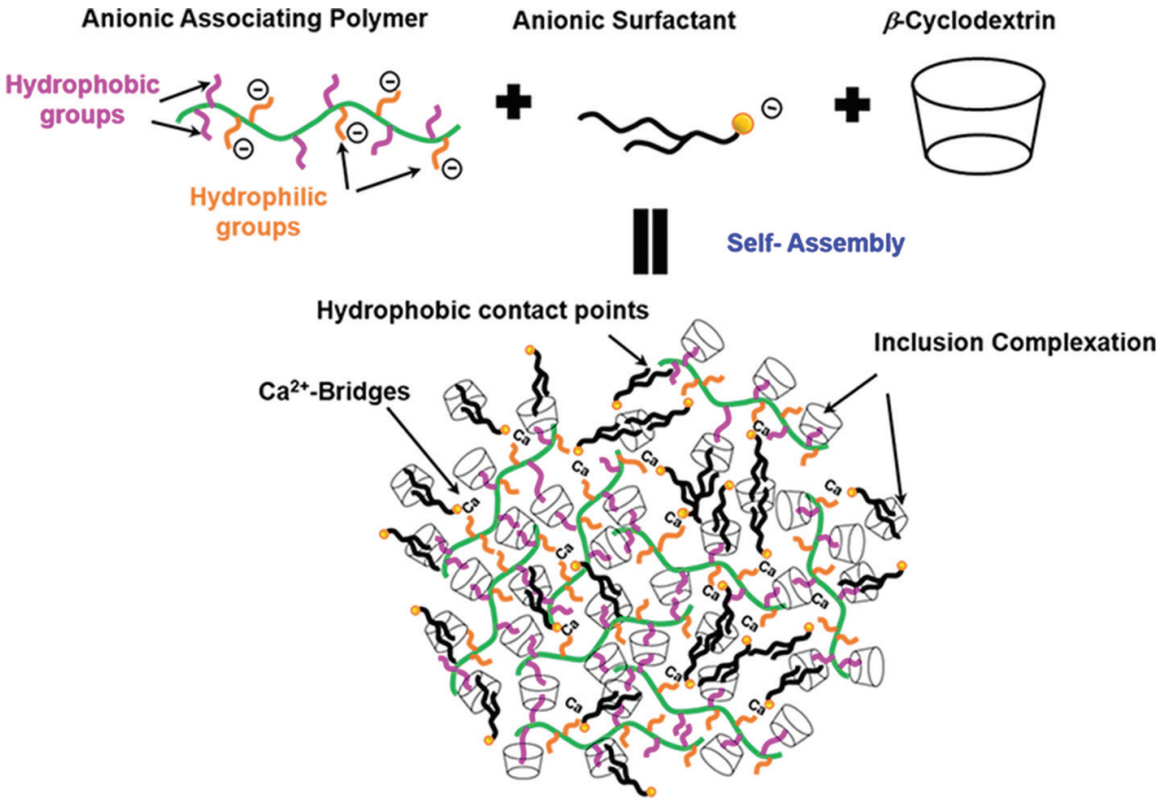

Figure 4. Hypothetical network structure via self-assembly among β-CD, associating polymer, and anionic surfactant in brine solution.

because the molecular locations containing the β-CD complexations become more hydrophilic in nature [7].

2.4. Effect of polymer concentration

Associating polymers contain hydrophobic pendant groups, which are important contact points between the hydrophobic tails of the surfactant and the cavity of the β-CD leading to the self-association and formation of supramolecular three-dimensional (3D) networks. Therefore, the effect of polymer concentration on the properties of the SAP-AP systems at a fixed concentration of surfactant and β-CD (i.e. optimum concentration: 70 ppm surfactant; 70 ppm β-CD) was established. The concentrations of polymer evaluated were 0.25, 0.5, and 0.75 wt%.

Figure 5(a–c) displays the results of the oscillatory tests for the optimum SAP-AP systems at different concentrations of the respective polymers AP1, AP2, and AP3. As polymer concentration increases, G' and G'' increase. A higher concentration of associating polymers increases the number of hydrophobic contact points, which promotes more intermolecular hydrophobic interactions, host-guest complexations, and other noncovalent associations (i.e. H- and Ca^{2+}-bridging). Additionally, higher polymer concentration enhances chain overlapping, which also contributes to the formation of a network of higher structural strength [13].

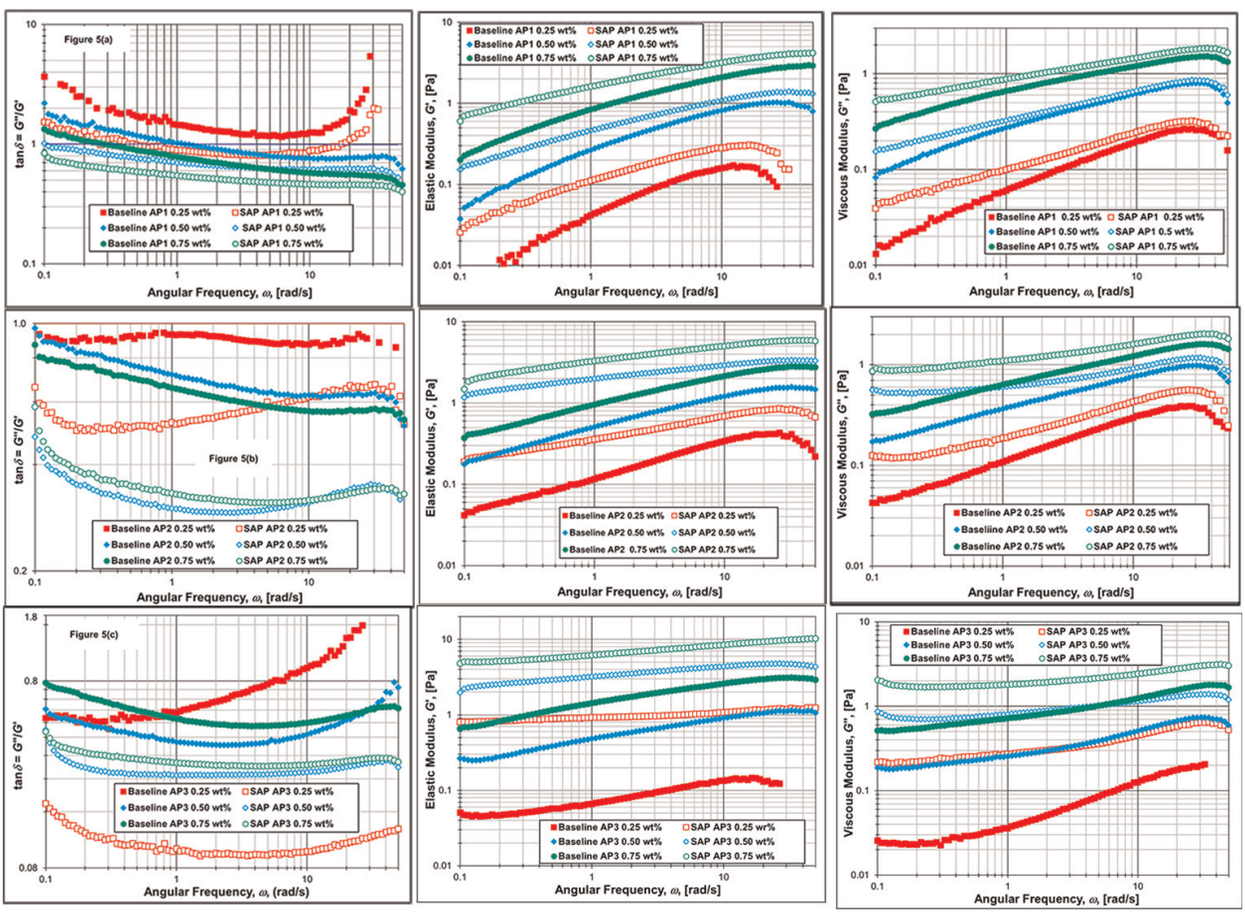

Figure 5. Oscillatory tests for the optimum SAP-AP systems at different concentrations of polymers: AP1, AP2, and AP3.

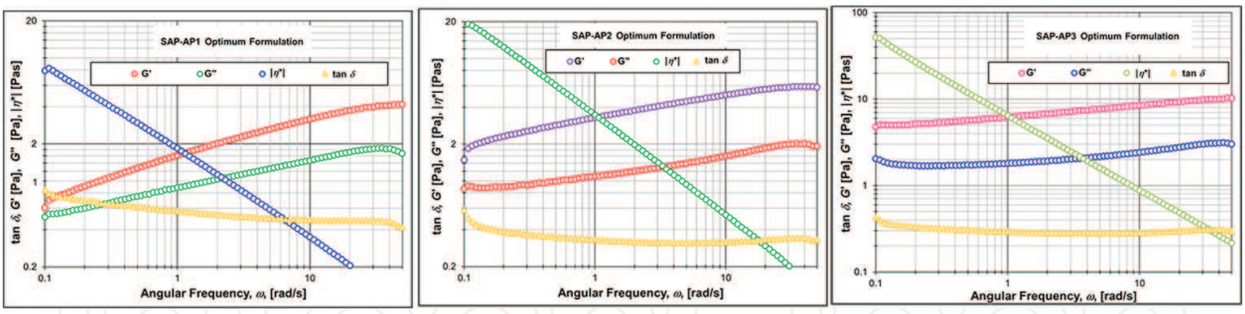

Figure 6. Frequency-dependent rheological performance of the optimum SAP-AP systems for polymers AP1, AP2, and AP3 in saline solution.

These results guided the selection of the optimum formulation of the SAP-AP system as follows, 0.75 wt% associating polymer (AP), 0.007 wt% (70 ppm) of surfactant, and 0.007 wt % (70 ppm) of β-CD prepared in saline solution. **Figure 6(a–c)** presents the frequency-dependent rheological performance of the optimum SAP-AP systems for polymers AP1, AP2, and AP3, respectively.

The frequency-dependent rheological data (**Figure 6**) indicates that these systems follow the typical behavior of three-dimensional network structures showing $G' > G''$ in the range of frequency studied [22]. As explained by Mezger, "the curves of G' and G'' often occur in the form of almost parallel straight lines throughout the entire frequency range showing a slight slope only" … "The shape of the curves [also indicates that these] … network structures are exhibiting a relatively constant structural strength in the whole frequency range" [22].

3. Effect of ionic strength on the SAP-AP systems

Salts significantly affect the viscosity of polymer solutions. The screening of the negatively charged moieties (i.e. carboxyl groups) in the polymer structure in the presence of mono- and divalent cations causes viscosity loss due to polymer coiling, polymer precipitation, and phase separation [2, 3, 5, 6, 23–25].

Figure 7(a–c) displays the results of the frequency sweeps of polymers AP1 and AP2 and their corresponding SAP-AP systems at the following brine concentrations: 1.4, 2.1, 4.2, 6.3, and 8.4 wt%. While for polymer AP3 and its corresponding SAP-AP3 system, the effect of ionic strength was evaluated at the following brine concentrations: 2.1, 4.2, 6.3, and 8.4 wt%.

In the case of polymer AP1, **Figure 7(a)** shows that it is strongly affected by salinity and hardness. As brine concentration increases, the tanδ-curve shifts from lower values toward medium range values, which means that the polymer flow behavior changes to a more viscoelastic liquid. G'', G', and $|\eta^*|$ decrease as salinity increases. This rheological behavior indicates that an increase in ionic strength weakens the hydrophobic interactions in the associating polymer resulting from the electrostatic screening of the charged segments [13] causing the coiling/folding of the polymer backbone.

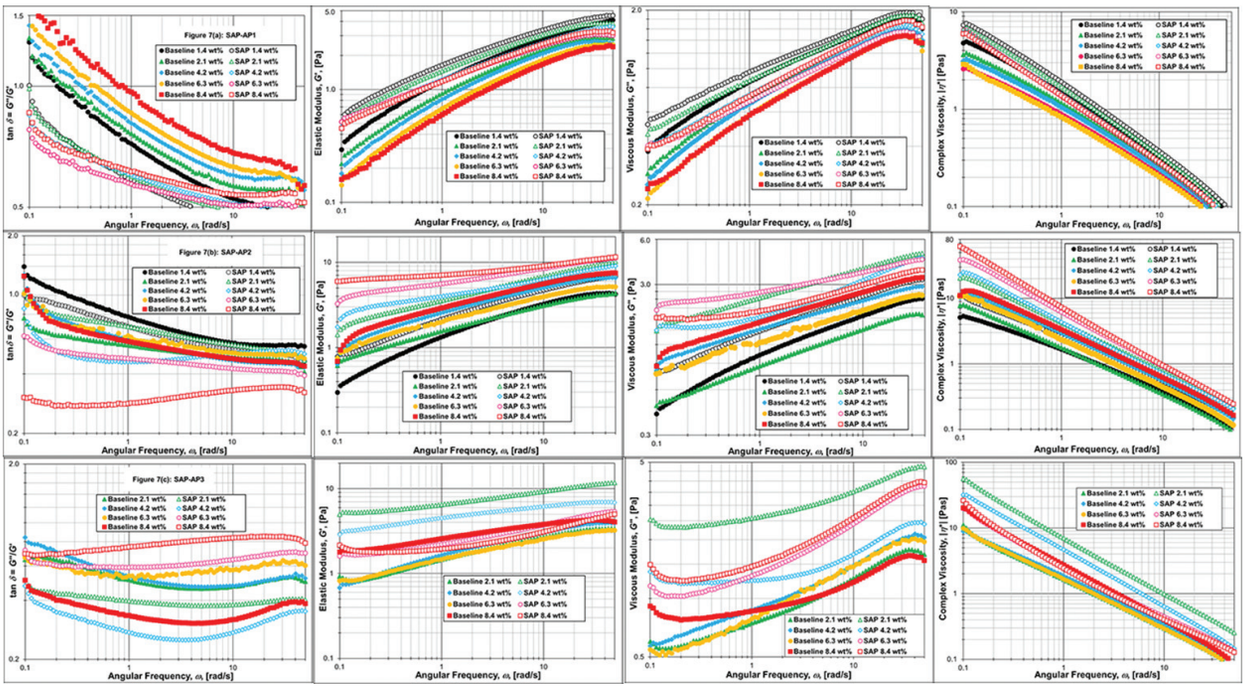

Figure 7. Frequency sweeps of polymers AP1, AP2, and AP3 and the corresponding SAP-AP systems at several brine concentrations at T = 25°C.

On the contrary, for the SAP-AP1 system, **Figure 7(a)** demonstrates that as salinity and hardness concentration increase, $G' > G''$ ($\tan\delta < 1$) throughout the entire frequency range; thus, in these systems, the elastic behavior dominates, which is characteristic of supramolecular aggregates [22]. Although as salinity concentration increases, G'', G', and $|\eta^*|$ decreases, the SAP-AP1 system displays higher structural strength relative to the AP1 polymer. Self-association seems to prevent electrostatic screening of the charged sections of the polymer molecule. Therefore, the SAP-AP1 system is less affected by electrostatic effects, which enhances its structural strength and functionality. Furthermore, the bulky size and shape of the β-CD molecules increase the steric hindrance that might diminish the electrostatic effects in these network structures [3, 13].

Figure 7(a) also shows that the SAP-AP1 prepared in the highest brine concentration of 8.4 wt% seems to collapse showing the same rheological behavior of the SAP-AP1 prepared in 6.3 wt% brine. These observations indicate that for the experimental conditions of this work, a brine concentration of 6.3 wt% seems to be the threshold before electrostatic effects become significant for this system.

The effect of salinity on the rheological behavior of polymer AP2 presented in **Figure 7(b)** is noticeably different than that for polymer AP1. In this case, it seems that increasing brine salinity and hardness strengthens the intermolecular hydrophobic interactions. The tanδ-values are shifted from $\tan\delta > 1$ (1.4 wt% brine) to $\tan\delta < 1$ (2.1 – 8.4 wt% brine) and the polymer attained a flow behavior of a physical network. G'-, G''-, and $|\eta^*|$-values increase

throughout the entire range of angular frequency as salinity and hardness concentrations increase. These results suggest that a higher content of hydrophobic groups in the AP2 polymer makes it less susceptible to electrostatic effects. **Figure 7(b)** makes evident that the SAP-AP2 system displays a better rheological performance than the baseline AP2. Again, an increase in the ionic strength causes a decrease in the tanδ-values. The SAP-AP2 prepared in 8.4 wt% brine shows the lowest tanδ-value. G', G'', and $|\eta^*|$ also increase with salinity and hardness concentration. The SAP-AP2 formulated in 6.3 and 8.4 wt% brine displays the highest values of complex viscosity, $|\eta^*|$. These observations demonstrate that an increase in the ionic strength reinforces the inter- and intramolecular forces building up the supramolecular SAP-AP2 system, which improves its viscosifying power [13].

Figure 7(c) presents the effect of salinity and hardness concentration on the rheological behavior of polymer AP3 and the SAP-AP3 system. **Figure 7(c)** demonstrates a negligible effect of brine salinity in the range from 2.1 to 6.3 wt% on the rheological properties of polymer AP3. In contrast, above this salinity range (i.e. brine 8.4 wt%), the rheological behavior of AP3 is significantly affected. For instance, the tanδ-curve shifts toward very low values and $G''/G' < 1$ in the entire range of angular frequency, which suggests the reinforcement of the intermolecular hydrophobic interactions generating a stronger physical network structure. These observations seem to indicate that the lower anionicity and larger hydrophobic content of the AP3 polymer improve its salt tolerance.

The viscoelasticity of the SAP-AP3 system is greater than the viscoelasticity of polymer AP3 at all salinity concentrations (see **Figure 7(c)**). At the lowest salinity concentration of 2.1 wt%, the SAP-AP3 system shows far superior rheological properties (i.e. enhanced viscosifying power and elasticity) in the entire angular frequency range. G', G'', and $|\eta^*|$ are significantly higher compared to the baseline. It seems that this salinity concentration (i.e. 2.1 wt%) greatly reinforces the strength of the inter- and intramolecular interactions taking place in this system. The G'-curve is almost parallel to the x-axis, which is typical of a highly stable structural network [22]. However, increasing the ionic strength beyond 2.1 wt% negatively affects the viscoelasticity of this system.

Overall, the SAP-AP systems are less sensitive to electrostatic effects compared to the AP polymers. The enhanced salt tolerance may result from the bulky size of the β-CD host-guest complexations that "sterically [hinders] the polymer chain so that the hydrodynamic radius does not fully collapse to a random coil configuration at high salinity" [6].

These experimental observations also indicate that the hydrophobic content in the associating polymers plays a vital role in the strength, rheological behavior, and ionic strength sensitivity of the SAP-AP systems. For instance, the SAP-AP system derived from the baseline polymer AP2, which has a medium content of hydrophobic groups, shows the formation of a stable supramolecular network highly functional in brines with high salinity and hardness concentration (i.e. brine 8.4 wt%). For this SAP-AP2 system, an increase in the ionic strength increases its elasticity and viscosifying power. This functionality is important for applications in enhanced oil recovery.

4. Effect of shear and ionic strength on the SAP-AP systems

Previous research has demonstrated that the mechanical degradation of polymers is path independent; thus, the effect of shear on the mechanical stability of polymers can be evaluated using any kind of degrading geometry [26]. In this work, the mechanical stability of the SAP-AP systems was determined through thixotropic behavior analysis using oscillatory rheology as recommended in Ref. [22]. **Table 3** summarizes the dynamic-mechanical conditions employed during the thixotropic analysis. The percentage of regeneration method was used to analyze the thixotropic behavior of the samples. In this method, the percentage of regeneration that takes place at the end of the third interval is read off and the percentage is calculated in relation to the reference value G'-at-rest at the end of the first interval which was taken as the 100% value [22]. These analyses were conducted for the baseline polymers and for the SAP-AP systems prepared at different salinity concentrations: 1.4, 2.1, 4.2, 6.3, and 8.4 wt% (see **Table 1**). The objective was to determine the simultaneous effect of shear and ionic strength on the structural and shear stability of the different systems.

Figures 8–10 summarize the time-dependent function of G' and G'' for Step 1 and Step 3 for polymers AP1 and SAP-AP1, AP2 and SAP-AP2, and AP3 and SAP-AP3, respectively. Likewise, **Tables 4** and **5** summarize the structural strength of the baseline polymers and the corresponding SAP-AP systems in terms of the G'- or G''-values taken at the end of Step 1, and the G'- or G''-values taken at the end of Step 3, and the percentage (%) of structural regeneration of the respective samples.

Steps	Oscillation test	ω (rad/s)	Strain (%)	Number of samples	Test time (s)
1	Single frequency/strain controlled	6.283	20 within the LVE	200	≈960
2	Single frequency/strain controlled	6.283	100 outside the LVE	100	≈480
3	Single frequency/strain controlled	6.283	20 within the LVE	200	≈960

LVE refers to the linear viscoelastic range.

Table 3. Preset of the dynamic-mechanical conditions for each of the intervals used during the thixotropic behavior analysis.

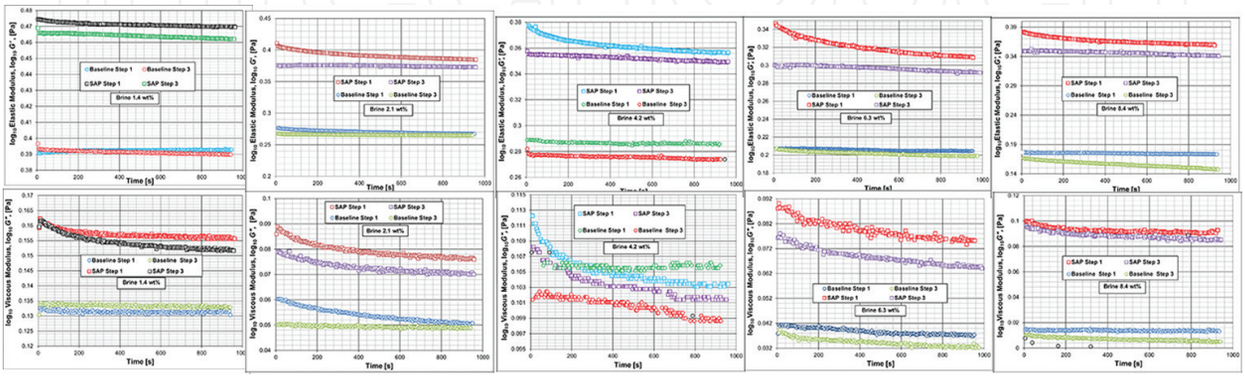

Figure 8. $\log_{10} G'$ and $\log_{10} G''$ for steps 1 and 3 vs. time for polymer AP1 and SAP-AP1.

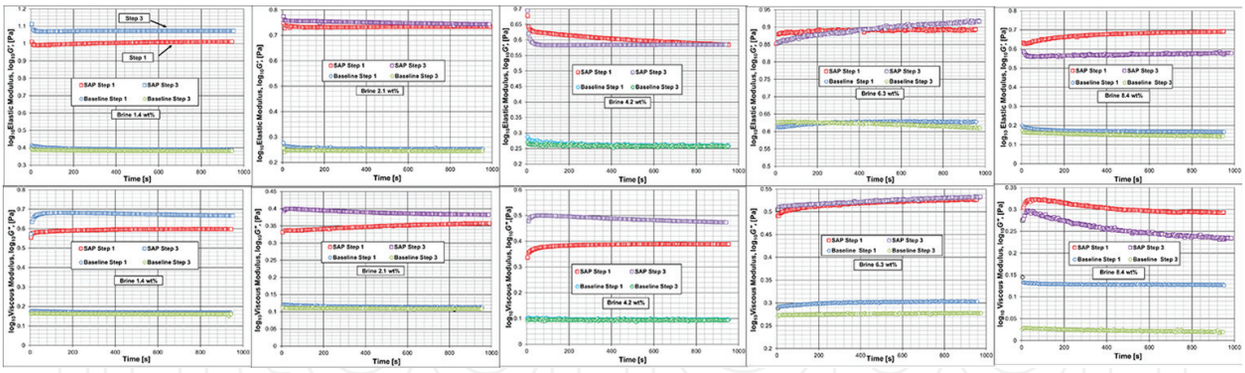

Figure 9. $\log_{10} G'$ and $\log_{10} G''$ for steps 1 and 3 vs. time for polymer AP2 and SAP-AP2.

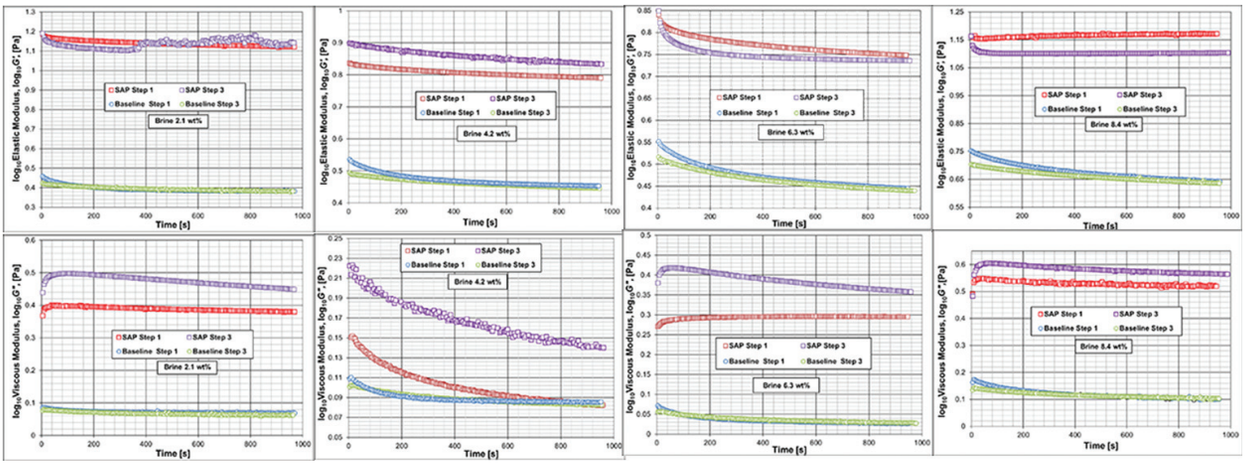

Figure 10. $\log_{10} G'$ and $\log_{10} G''$ for steps 1 and 3 vs. time for polymer AP3 and SAP-AP3.

Figure 8 demonstrates that the optimum SAP-AP1 shows higher structural strength (> G'-values and > G''-values) relative to polymer AP1. The second important result is that there is no complete regeneration of the initial structural strength. The first two rows of **Table 5** show that the percentage of structural regeneration for polymer AP1 in terms of $G' > 95\%$ for all brine salinities (1.4, 4.2, 6.3 wt%) except for the 8.4 wt% brine with a structural regeneration of 91%. In terms of G'' (see **Table 5**), both systems: AP1 and SAP-AP1 show a structural regeneration > 96%, excluding the baseline polymer AP1 in 1.4% brine that shows a gain in structural strength with a regeneration of $G'' > 100\%$.

The minor loss of structural strength observed for both systems might be related to macromolecular shear degradation under the high-shear forces applied during Step 2 causing the breaking of carbon/carbon bonds of some of the polymer chains [5].

Figure 9 presents the time-dependent behavior of polymer AP2 and the SAP-AP2 system in terms of G' and G'' for the low-shear interval (Step 1) and for the regeneration interval (Step 3). Experimental trends observed from **Figure 9** and **Tables 4** and **5** are as follows:

	Brine concentration (wt%)									
	1.4		**2.1**		**4.2**		**6.3**		**8.4**	
	***G′* (Pa)**	**Reg (%)**	***G′* (Pa)**	**Reg (%)**	***G′* (Pa)**	**Reg (%)**	***G′* (Pa)**	**Reg (%)**	***G′* (Pa)**	**Reg (%)**
Polymer AP1										
Step 1	2.47		1.92		1.82		1.59		1.49	
Step 3	2.34	**98.84**	1.85	**96.51**	1.80	**98.82**	1.57	**98.59**	1.36	**91.03**
SAP-AP1										
Step 1	3.05		2.50		2.28		2.04		2.18	
Step 3	3.01	**98.49**	2.42	**96.75**	2.25	**98.34**	1.99	**97.72**	2.17	**99.7**
Polymer AP2										
Step 1	2.45		1.86		1.82		—		1.07	
Step 3	2.41	**98.16**	1.72	**92.47**	1.82	**100**	—	**—**	1.04	**97.70**
SAP-AP2										
Step 1	10.26		6.05		3.61		—		4.92	
Step 3	11.82	**>100**	6.20	**>100**	3.61	**100**	—	**—**	3.79	**77.01**
Polymer AP3										
Step 1	—		2.41		2.84		2.79		4.38	
Step 3	—	**—**	2.41	**100**	2.79	**98.27**	2.75	**98.82**	4.33	**98.68**
SAP-AP3										
Step 1	—		13.22		6.17		5.60		14.85	
Step 3	—	**—**	13.86	**>100**	6.81	**>100**	5.45	**97.23**	12.68	**85.39**

The objective of bold numbers in Table 4 is to emphasize the percentage of regeneration in each system.

Table 4. *G′*-values and percentage of regeneration.

- The SAP-AP2 system formulated at different ionic strengths displays significantly higher structural strength, *G′* and *G″*, than the baseline AP2 polymer.
- As the ionic strength increases, the structural strength of the AP2 polymer and the SAP-AP2 system decreases.
- The baseline polymer AP2 shows structural regeneration *G′* and *G″* > 92% but < 100% in the range of salinity concentration studied. While the SAP-AP2 systems prepared in 1.4, 2.1, and 4.2 wt% brines display gain in structural strength with regenerations ≥ 100%. In 8.4 wt% brine, the structural regeneration SAP-AP2 system falls to 77% and to 87.26% in terms of *G′* and *G″*, respectively.

The gain in structural strength is significant for the SAP-AP2 prepared in low brine salinity with a 15% gain of the *G′*-value and 17% gain of the *G″*-value (see **Figure 9**). Although at brine salinity concentrations up to 4.2 wt%, the gain in structural strength is ≥ 100%, it decreases as salinity increases, which demonstrates the negative effect of increased ionic strength on the shear stability of the SAP-AP2 system.

	Brine concentration (wt%)									
	1.4		**2.1**		**4.2**		**6.3**		**8.4**	
	***G″* (Pa)**	**Reg (%)**	***G″* (Pa)**	**Reg (%)**	***G″* (Pa)**	**Reg (%)**	***G″* (Pa)**	**Reg (%)**	***G″* (Pa)**	**Reg (%)**
Polymer AP1										
Step 1	1.311		1.14		1.28		1.05		1.03	
Step 3	1.371	**>100**	1.10	**96.92**	1.25	**97.66**	1.04	**98.89**	1.02	**99.03**
SAP-AP1										
Step 1	1.47		1.23		1.27		1.14		1.18	
Step 3	1.46	**99.25**	1.21	**98.17**	1.26	**99.2**	1.12	**98.29**	1.17	**99.07**
Polymer AP2										
Step 1	1.476		1.39		1.27		—		1.34	
Step 3	1.447	**98.2**	1.28	**98.54**	1.27	**100**	—	**—**	1.29	**96.26**
SAP-AP2										
Step 1	3.96		2.72		2.45		—		1.97	
Step 3	4.64	**>100**	2.91	**>100**	2.99	**>100**	—	**—**	1.72	**87.26**
Polymer AP3										
Step 1	—		1.172		1.22		1.07		1.26	
Step 3	—	**—**	1.155	**98.55**	1.21	**98.27**	1.07	**100**	1.27	**>100**
SAP-AP3										
Step 1	—		2.39		1.209		1.97		3.30	
Step 3	—	**—**	3.16	**>100**	1.381	**>100**	2.28	**>100**	3.67	**>100**

Table 5. *G″*-values and percentage of regeneration.

The mechanical stability shown by the SAP-AP2 system might result from the increased rigidity of the polymeric network due to self-aggregation with the bulky structure of the β-CD and the long-chain alkyl branched anionic surfactant [3, 5]. Supramolecular aggregates based on physical bonding are considerably more rigid compared to the superstructures of the thread-like macromolecules of synthetic polymers [22].

Figure 10 indicates that the SAP-AP3 system displays higher structural strength in terms of *G′* and *G″* relative to the baseline polymer. In low-salinity brines (≤ 4.2 wt%), the SAP-AP3 systems show a gain in the structural strength (see *G′*- and *G″*-curves in **Figure 10**). However, for brine salinities ≥ 4.2 wt%, there is no complete structural regeneration as shown by the *G′*-curve.

The gain in structural strength displayed by the SAP-AP2 and the SAP-AP3 systems in salinity concentrations ≤ 4.2 wt% demonstrates the self-healing character of these self-assemblies. As stated by Yang, "supramolecular self-healing materials [rely] on the use of noncovalent bonds to generate reversibility and dynamic networks, which are able to heal the damaged sites" [10]. According to Mezger, (this self-healing or self-repairing effect occurs because) "the structural development aims at achieving a balance or equilibrium of the active forces or energies …

based on the very fast connection, disconnection, and re-connection" of the physical bonds such as the decomplexation and complexation of host-guest interactions [7, 22], that results in improved structural strength. "Therefore, when tension is imparted on these networks, the force is distributed homogeneously across the whole network [due to the dynamic disassembling and re-assembling of the physical interactions]" protecting the macromolecules in the network from permanent shear degradation [7].

5. Thermal stability of the SAP-AP systems

Thermal degradation of polymer leads to chemical changes of the polymer structure. For instance, in the case of polymers derived from polyacrylamides, high temperatures induce the hydrolyzation of the acrylamide group to the acrylate moiety. These hydrolysis reactions are strongly correlated to temperature; thus, the higher the temperature, the higher the hydrolysis [2]. In this study, both short- and long-term thermal stabilities of the AP polymers and the corresponding SAP-AP systems were evaluated.

5.1. Short-term thermal stability

The AP polymers and the corresponding optimum SAP-AP systems were subjected to dynamic-mechanical thermo-analysis or DMTA. In this analysis, the dynamic temperature sweep was conducted by using a linear heating rate (8.65°C/min) from 9 to 81°C (±0.2°C) as an upward ramp immediately followed by a linear cooling rate (7.3°C/min) from 81 to 9°C (±0.2°C) as a downward ramp. In these tests, the angular frequency (ω) was fixed at 7 rad/s, while the strain was fixed at 20% (within the LVE range). **Figure 11** displays the temperature-dependent functions of G', G'', and tanδ for polymer AP1 and the SAP-AP1 system for low (2.1 wt%)- and high (8.4 wt%)-concentration salinity; while **Figure 12** presents the temperature-dependent functions of G', G'', and tanδ for polymers AP2 and AP3 and their corresponding SAP-AP systems in 8.4 wt % brine concentration.

At low-ionic strength (i.e. 2.1 wt% brine), the SAP-AP1 system shows higher structural strength in terms of G' and G'' relative to polymer AP1. The SAP-AP1 system displays a tan$\delta < 1$ (i.e. $G' > G''$) in the entire range of temperature that is consistent with the behavior of network structures. At low temperatures, the tanδ-curve of the AP1 polymer shows tan$\delta < 1$, as temperature increases the crossover point ($G' = G''$) is reached and the tanδ-curve is shifted to a value of tan$\delta > 1$ at higher temperatures, which corresponds to the behavior of viscoelastic liquids. The cooling curves of tanδ, G', and G'' as a function of temperature demonstrate a decreasing structural strength of the polymer systems relative to the corresponding heating curves. According to Mezger, as temperature increases, "the [polymer] molecules are able to move along one another which results in an increasing number of disentanglements. With increasing temperature, more motion occurs between the molecules which again cause an increase in the amount of the frictional forces [that produces] frictional heat that afterward is lost for the sample in the form of thermal energy … This process can be observed as a decreasing G'' value" [22]. The cooling temperature curve displays indeed lower G''-values. Likewise, for the SAP-AP1 system, with increasing temperature, dissociation and/or disassembling of the

http://dx.doi.org/10.5772/intechopen.74618

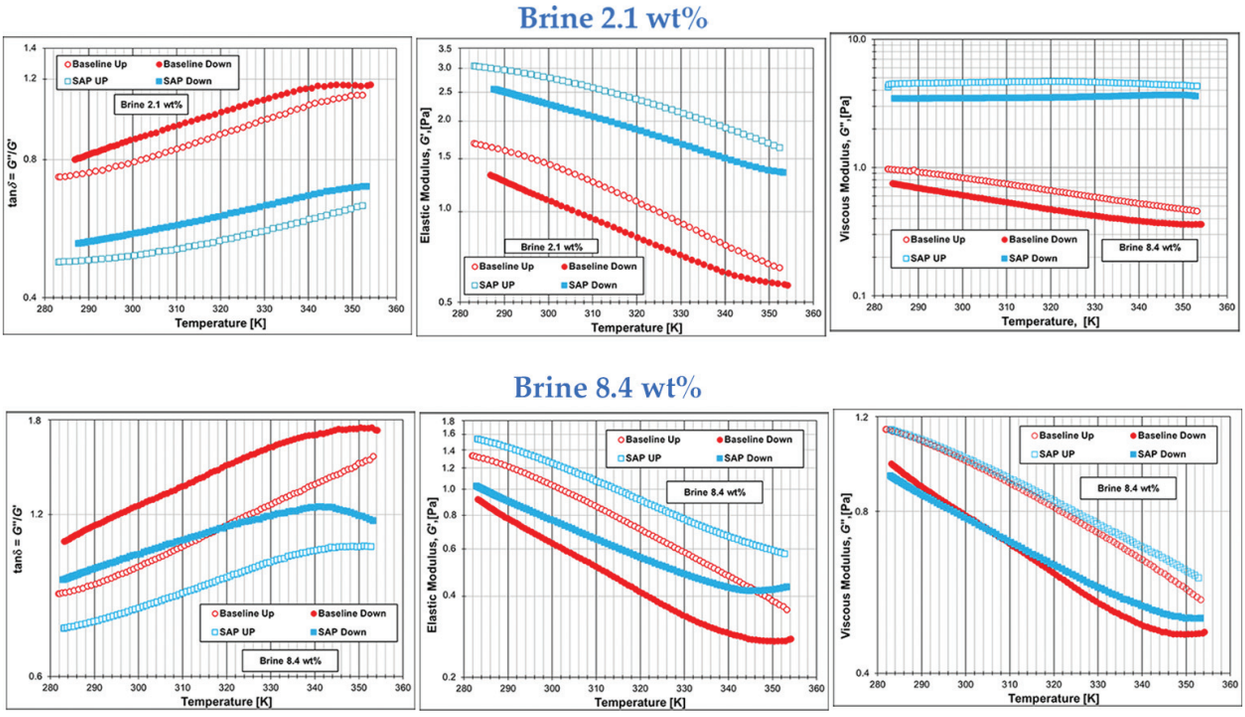

Figure 11. Temperature-dependent functions of G', G'', and tanδ for polymer AP1 and SAP-AP1 system.

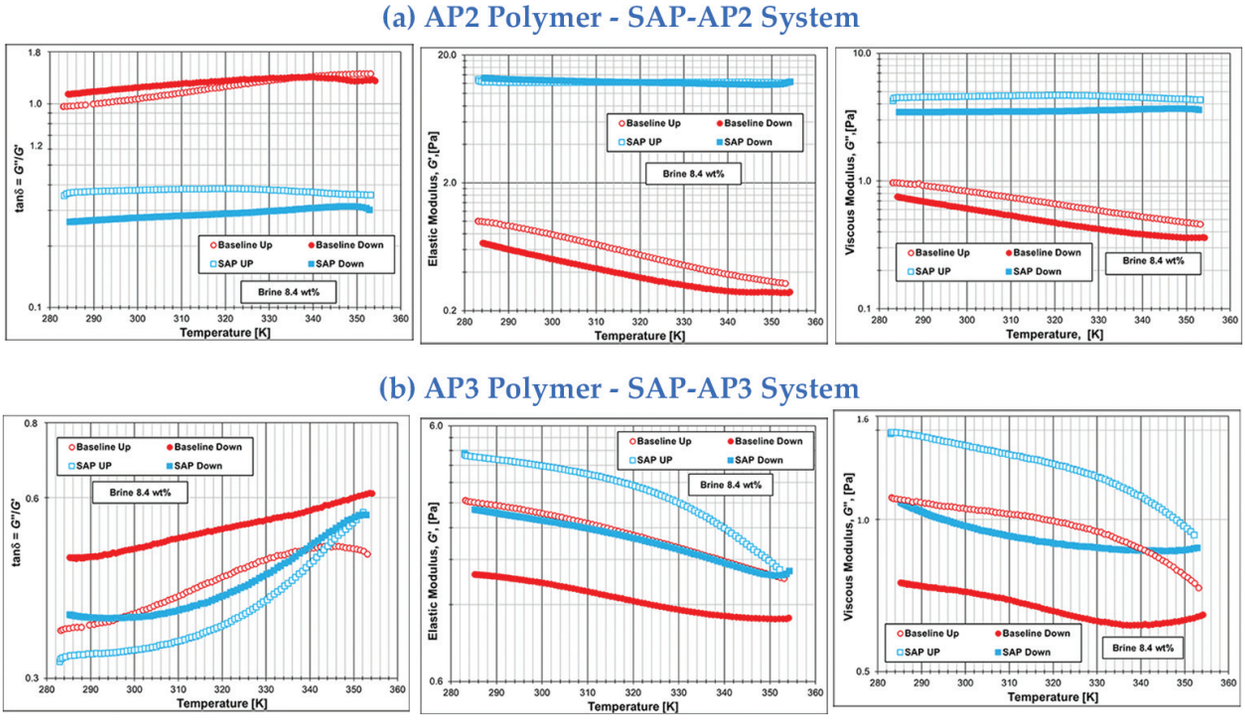

Figure 12. Temperature-dependent functions of G', G'', and tanδ for polymers AP2 and AP3 and systems SAP-AP2 and SAP-AP3.

physical interactions takes place. Therefore, "the superstructure [network] yields more and more, breaking increasingly into smaller parts, turning into a state of flexibility. Later, during the cooling process, the physical bonds are reformed, and the network structure regains

rigidity. However, due to losses of frictional heat in the form of thermal energy, a decrease of the G''-values is observed in the cooling temperature curve" [22].

Increasing the ionic strength (brine 8.4 wt%) and temperature significantly affects the structural strength of polymer AP1 and the SAP-AP1 system (see **Figure 11**). Similarly, the downward curve (i.e. cooling process) shows a decreasing structural strength relative to the corresponding heating curves. The SAP-AP1 temperature curve shows a higher structural strength in terms of G'-values compared to the AP1 polymer; however, in terms of G''-values, there is no difference between the AP1 polymer and the SAP-AP1 system. Furthermore, the tanδ-curve of the cooling process for the SAP-AP1 system shows a shift from tanδ-values > 1 at elevated temperatures to tanδ-values < 1 at lower temperatures. This makes evident that at elevated temperatures, the SAP-AP1 network system changes its flow behavior, showing $G'' > G'$, performing as a viscoelastic liquid. As temperature decreases, the network becomes more rigid and the tanδ-values become < 1, showing again the consistency of a rigid supramolecular structure.

At elevated ionic strength (i.e. 8.4 wt% brine), the baseline polymers AP2 and AP3 and their corresponding SAP-AP systems show similar behavior to the baseline AP1 and SAP-AP1, discussed above. Nevertheless, it is important to mention that the SAP-AP2 system shows the highest structural strength in terms of G' and G'' and the least hysteresis between the heating and the cooling curves among the systems. These observations make evident that the optimum SAP-AP2 displays enhanced structural strength at elevated temperatures and ionic strengths compared to the baseline.

5.2. Long-term thermal stability

The AP and SAP-AP systems were subjected to a thermal stability test at 90°C for a period of 8 weeks. The presence of dissolved oxygen at high temperatures might induce the formation of free radicals which degrade the polymer molecule by cleavage reducing its molecular weight and viscosifying functionality [2]. Besides, if dissolved oxygen is present in the polymer solutions together with very low concentrations of dissolved iron, it might also cause substantial polymer degradation [4, 26–30]. Therefore, to prevent chemical degradation, the AP and the SAP-AP samples were placed in a glove chamber and bubbled with nitrogen at a pressure ranging from 10 to 20 psi for a period of 30 min. Two duplicated set of samples of the AP and the SAP-AP systems were prepared in two different brine salinity concentrations: 2.1 and 8.4 wt% and placed in the oven at 90 ± 0.5°C for 8 weeks. Every 2 weeks, a set of samples were taken out of the oven and subjected to rheological analysis. **Figure 13** displays the G'- and G''-curves as a function of angular frequency and time for the AP and SAP-AP systems at brine salinity concentrations of 2.1 and 8.4 wt%.

The G'- and G''-plots in **Figure 13** demonstrate that the AP polymers and the SAP-AP systems are significantly degraded at a temperature of 90°C after 2 weeks of testing. A dramatic drop of G' and G'' is observed for all the samples in both low and high salinities.

In low-salinity brine, samples AP1, AP2, SAP-AP1, and SAP-AP2 show precipitation of solids and color change at week # 4; while in samples AP3 and SAP-AP3, the precipitation of solids was observed at week # 8. In high-salinity brine, precipitation of solids took place faster at week # 2.

http://dx.doi.org/10.5772/intechopen.74618

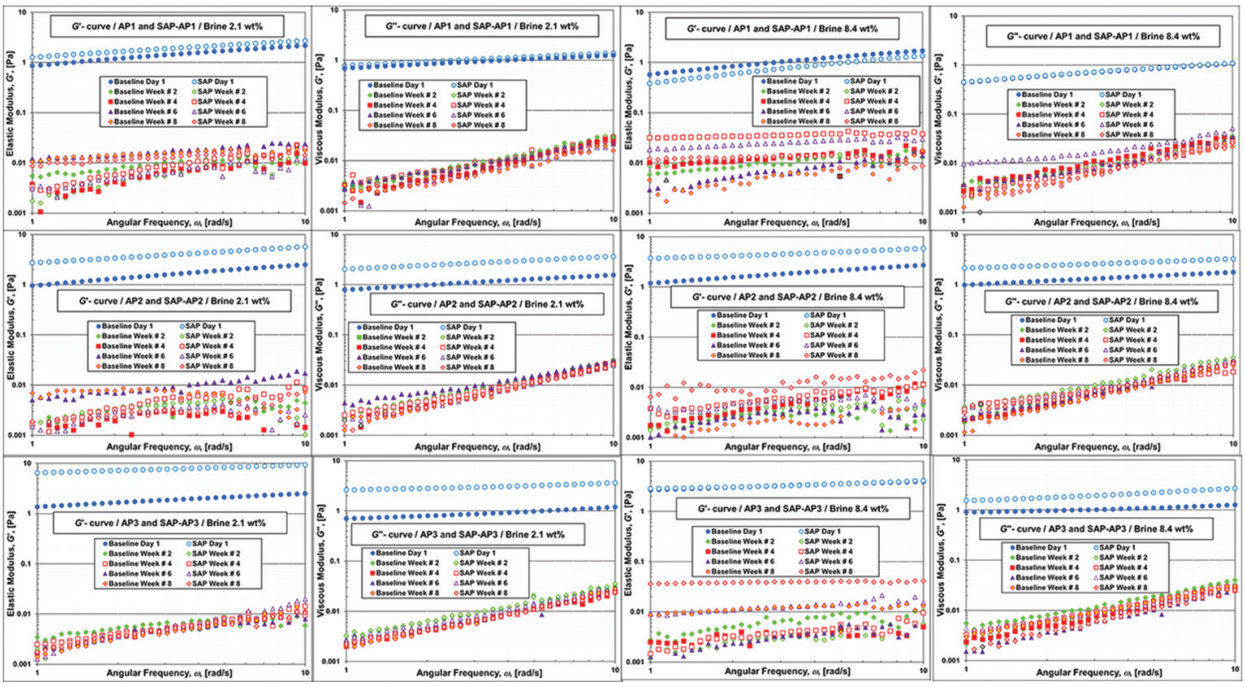

Figure 13. *G′*- and *G″*-curves vs. angular frequency, time, and brine salinity.

These observations clearly indicate the combined damaging effect of salinity and elevated temperature on the stability of the AP and SAP-AP systems.

Although the introduction of hydrophobic groups into the molecular chain is an effective way to improve polymer salt tolerance and thermal stability [3], these hydrophobic moieties such as AMPS or n-VP are still susceptible to hydrolysis at high temperatures (i.e. > 85°C). As explained by Levitt and Pope, "…hydrolysis of the [amide] group from the acrylamide moiety and/or β, β, dimethyl taurine from the AMPS moiety [takes place] forming additional acrylate moiety in the hydrolysed polymer molecule" [6]. At high salinity and hardness concentration, these acrylate moieties (i.e. hydrolyzed poly(AM-co-AMPS)) associate strongly with cations (i.e. Ca^{2+}, M^{2+}) and polymer precipitation takes place, which results in a rapid drop of viscosity of the polymer solution that becomes turbid [6, 31]. Precipitation of polymer due to interactions with multivalent cations increases with temperature. Furthermore, thermal degradation of polymers results in a "reduction of molecular weight because of free-radical induced scission of the acrylic backbone" [6].

This long-term thermal stability testing demonstrates that the AP and the SAP-AP systems are not stable at elevate temperatures; therefore, these SAP-AP systems are recommended for low-temperature (< 90°C) applications.

6. Conclusions

In summary, we formulated advanced polymer-surfactant systems via self-assembling driven by host-guest chemistry and other physical noncovalent bonding by mixing associating

polymers, with an anionic surfactant, and β-CD in brine solutions. The optimum supramolecular systems were subjected to rheological characterization and several stability testing techniques to establish their tolerance to increasing ionic strength concentration, shear degradation, and thermal stability. The most significant findings are outlined as follows:

- The formulated SAP-AP systems show remarkable gain of viscoelastic properties and elevated structural strength relative to the associating baseline polymers.
- The SAP-AP network structures are less sensitive to electrostatic effects than the corresponding baseline polymers AP1, AP2, and AP3. The increase in salt tolerance may be aided by the steric effect of the β-CD host-guest complexations acting as large rigid groups within the supramolecular network that prevents the collapse and/or coiling of the polymer chain at elevated ionic strength. This functionality is important for EOR applications.
- The SAP-AP systems show remarkable shear stability relative to the baseline polymers. If the high-shear forces imposed on the network structures are lifted and as soon as the equilibrium of the shear forces and the flow resistance forces is reached, the SAP-AP systems show high structural regeneration, which is > 95% for the case of the SAP-AP1 system; while the SAP-AP2 and SAP-AP3 systems display a gain of structural strength with regeneration > 100%. The gain in structural strength evidences the self-healing performance of these SAP-AP self-assemblies. The overall trend is that increasing the hydrophobic content of the associating polymers increases the shear stability and the structural strength of the supramolecular formulations.
- The short-term thermal stability testing demonstrates that all SAP-AP systems display higher structural strength in terms of G' and G'' when compared to the corresponding baseline polymers in the entire range of temperature and ionic strength evaluated.
- The long-term thermal stability testing carried out at 90°C for a period of 8 weeks demonstrates that the AP polymers and the optimum SAP-AP systems are not stable at elevated temperatures; therefore, these systems are recommended for low-temperature ($\ll$ 90°C) applications.

Acknowledgements

The authors would like to extend their appreciation to Grace Hicks and Tayler Hunt from the Chemical Engineering Department, University of New Brunswick, for their technical involvement during the rheological evaluation of the SAP-AP systems. The authors are grateful to Sasol Chemicals and SNF Floerger for providing surfactant and polymer samples. Financial support from the University of New Brunswick through the Sabbatical Research Grant and the Canada Foundation for Innovation (CFI) is also acknowledged.

Author details

Laura Romero-Zerón* and Xingzhi Jiang

*Address all correspondence to: laurarz@unb.ca

Chemical Engineering Department, University of New Brunswick, Fredericton, New Brunswick, Canada

References

[1] Kang PS, Lim JS, Huh C. A novel approach in estimating shear-thinning rheology of HPAM and AMPS polymers for enhanced oil recovery using artificial neural network. In: The Twenty-third International Offshore and Polar Engineering Conference (ISOPE-I-13-171); Jun 30–Jul 5, 2013. Anchorage, Alaska: 2013. pp. 81-85

[2] Vermolen E, Van Haasterecht MJ, Masalmeh SK, Faber MJ, Boersma DM, Gruenenfelder MA. Pushing the envelope for polymer flooding towards high-temperature and high-salinity reservoirs with polyacrylamide based ter-polymers. In: SPE Middle East Oil and Gas Show; September 25–28, 2011; Manama, Bahrain: 2011. pp. 1-9

[3] Wu Y, Mahmoudkhani A, Watson P, Fenderson TR, Nair M. Development of new polymers with better performance under conditions of high temperature and high salinity. In: SPE EOR Conference at Oil and Gas West Asia; April 16–18, 2012; Muscat, Oman: 2012. pp. 1-11

[4] Sheng JJ, Leonhardt B, Azri N. Status of polymer-flooding technology. Journal of Canadian Petroleum Technology. 2015;**54**(02):16-26

[5] Zaitoun A, Makakou P, Blin N, Al-Maamari RS, Al-Hashmi AA, Abdel-Goad M. Shear stability of EOR polymers. SPE Journal. 2012;**17**(02):335-339

[6] Levitt D, Pope GA. Selection and screening of polymers for enhanced-oil recovery. In: SPE Symposium on Improved Oil Recovery; April 19–23, 2008; Tulsa, Oklahoma: pp. 1-18

[7] Tan S, Ladewig K, Fu Q, Blencowe A, Qiao GG. Cyclodextrin-based supramolecular assemblies and hydrogels: Recent advances and future perspectives. Macromolecular Rapid Communications. 2014;**35**(13):1166-1184

[8] Hu J, Liu S. Engineering responsive polymer building blocks with host–guest molecular recognition for functional applications. Accounts of Chemical Research. 2014;**47**(07):2084-2095

[9] Adler-Abramovich L, Gazit E. The physical properties of supramolecular peptide assemblies: From building block association to technological applications. Chemical Society Reviews. 2014;**43**(20):6881-6893

[10] Yang L, Tan X, Wang Z, Zhang X. Supramolecular polymers: Historical development, preparation, characterization, and functions. Chemical Reviews. 2015;**115**(15):7196-7239

[11] Dong R, Zhou Y, Huang X, Zhu X, Lu Y, Shen J. Functional supramolecular polymers for biomedical applications. Advanced Materials. 2015;**27**(03):498-526

[12] Hart LR, Harries JL, Greenland BW, Colquhoun HM, Hayes W. Supramolecular approach to new inkjet printing inks. Applied Materials & Interfaces. 2015;**7**(16):8906-8914

[13] Perttamo EK. Characterization of associating polymer (AP) solutions. Influences on flow behavior by the degree of hydrophobicity and salinity [thesis]. The University of Bergen; 2013

[14] SNF Floerger. Enhancing Polymer Flooding Performance. 30 Years of Experience in EOR [Internet]. 2017. Availble from: http://www.snfoil.com/images/phocagallery/brochures/SNF_in_chemical_enhanced_oil_recovery.pdf [Accessed: August 2, 2017]

[15] Sasol. Product Application Areas. Surfactants for Enhanced Oil Recovery Bulletin [Internet]. 2017. Available from: http://sasolnorthamerica.com/Images/Interior/productsearch-documents/eor%20bulletin%20sept%2025%202013.pdf [Accessed: August 2, 2017]

[16] Wassmuth FR, Hodgins LA, Schramm LL, Kutay SM. Screening and coreflood testing of gel foams to control excessive gas production in oil wells. SPE Reservoir Evaluation & Engineering. 2001;**4**(03):187-194

[17] Wei B, Romero-Zerón L, Rodrigue D. Novel self-assembling polymeric system based on a hydrophobic modified copolymer: Formulation, rheological characterization, and performance in enhanced heavy oil recovery. Polymers for Advanced Technologies. 2014;**25**(07): 732-741

[18] Wei B, Romero-Zerón L, Rodrigue D. Evaluation of two new self-assembly polymeric systems for enhanced heavy oil recovery. Industrial and Engineering Chemistry Research. 2014;**53**(43):16600-16611

[19] Wei B, Romero-Zerón L, Rodrigue D. Improved viscoelasticity of xanthan gum through self-association with surfactant: β-cyclodextrin inclusion complexes for applications in enhanced oil recovery. Polymer Engineering and Science. 2015;**55**(03):523-532

[20] Wei B, Romero-Zerón L, Rodrigue D. Formulation of a self-assembling polymeric network system for enhanced oil recovery applications. Advances in Polymer Technology. 2014;**33**(03):21413 (1–12)

[21] Herbst F, Döhler D, Michael P, Binder WH. Self-healing polymers via supramolecular forces. Macromolecular Rapid Communications. 2013;**34**(03):203-220

[22] Mezger TG. The Rheology Handbook: For Users of Rotational and Oscillatory Rheometers. 3rd ed. Hanover, Germany: Vincentz Network GmbH & Co KG; 2011

[23] Ayirala SC, Uehara-Nagamine E, Matzakos AN, Chin RW, Doe PH, van den Hoek PJ. A designer water process for offshore low salinity and polymer flooding applications. In: SPE Improved Oil Recovery Symposium; April 24–28, 2010; Tulsa, Oklahoma; 2010. pp. 1-12

[24] Han B, Lee J. Sensitivity analysis on the design parameters of enhanced oil recovery by polymer flooding with low salinity waterflooding. In: The Twenty-fourth International Ocean and Polar Engineering Conference; June 15–20, 2014; Busan, Korea: 2014. pp. 147-151

[25] Khorsandi S, Qiao C, Johns RT. Displacement efficiency for low-salinity polymer flooding including wettability alteration. SPE Journal. 2017;**22**(02):417-30

[26] Rivas C, Gathier F. C-EOR projects—offshore challenges. In: The Twenty-Third International Offshore and Polar Engineering Conference (ISOPE); June 30–July 5, 2013; Anchorage, Alaska: 2013

[27] Jouenne S, Anfray J, Levitt D, Souilem I, Marchal P, Lemaitre C, Choplin L, Nesvik J, Waldman T. Degradation (or lack thereof) and drag reduction of HPAM solutions during transport in turbulent flow in pipelines. Oil and Gas Facilities. 2015;**4**(01):80-92

[28] Seright R, Skjevrak I. Effect of dissolved iron and oxygen on stability of hydrolyzed polyacrylamide polymers. SPE Journal. 2015;**20**(03):433-441

[29] Manichand RN, Let MS, Kathleen P, Gil L, Quillien B, Seright RS. Effective propagation of HPAM solutions through the Tambaredjo reservoir during a polymer flood. SPE Production & Operations. 2013;**28**(04):358-368

[30] Jouenne S, Klimenko A, Levitt D. Polymer flooding: Establishing specifications for dissolved oxygen and iron in injection water. SPE Journal. 2017;**22**(02):438-446

[31] Levitt DB. The optimal use of enhanced oil recovery polymers under hostile conditions [Doctoral dissertation]. Austin: The University of Texas; 2009

IntechOpen